Results in Physics 9 (2018) 1250–1255

Contents lists available at ScienceDirect

Results in Physics

journal homepage: www.elsevier.com/locate/rinp

Axisymmetric flow of Casson fluid by a swirling cylinder

Muhammad Faisal Javed[a], Muhammad Imran Khan[b], Niaz Bahadur Khan[c,*], Riaz Muhammad[d], Muftooh Ur Rehman[d], Sajjad Wali Khan[e], Tufail A. Khan[f]

[a] Department of Civil Engineering, Sarhad University of Science and Information Technology, Peshawar, Pakistan
[b] Heriot Watt University, Edinburgh Campus, Edinburgh EH14 4AS, United Kingdom
[c] School of Mechanical and Manufacturing Engineering, National University of Science and Technology, Islamabad, Pakistan
[d] Department of Mechanical Engineering, CECOS University of IT and Emerging Sciences, Peshawar, Pakistan
[e] Civil Engineering Department, UET Peshawar, Pakistan
[f] Department of Basic Sciences, University of Engineering & Technology, Peshawar, Pakistan

ARTICLE INFO

Keywords:
Casson fluid
Heat generation/absorption
Swirl velocity
MHD
Stretched cylinder

ABSTRACT

The present communication aims to investigate the influence of heat generation/absorption on axisymmetric Casson liquid flow over a stretched cylinder. Flow is caused due to torsional motion of cylinder. The governing physical problem is modelled and transferred into set of coupled nonlinear ordinary differential equations. These equations are solved numerically using built-in-Shooting method. Influence of sundry variables on the swirling velocity, temperature, coefficient of skin friction and heat transfer rate are computed and analyzed in a physical manner. Magnitude of axial skin friction is enhances for larger Reynold number and magnetic parameter while local Nusselt number decays with the enhancement of Casson parameter, heat generation/absorption and magnetic parameter. Comparison with already existing results is also given in the limiting case.

Introduction

The analysis of non-Newtonian liquids is very important due to their applications in the industries and engineering. Soups, jams, china clay, synthetic lubricants, blood at low shear rate etc. are the examples of non-Newtonian liquids. The properties of such fluids cannot be described by a single constitutive equation. Nonlinear relationship exists between the rate of strain and stress for such liquids. Therefore different models of non-Newtonian liquids are described by the engineers and scientists (see [1–10]). Casson liquid is a non-Newtonian liquid which exhibits the shear characteristics and quantifies yield stress and high viscosity. When wall stress is larger than the yield stress, then such model is reduced to a Newtonian liquid. This model describes the behavior of various materials for example biological materials, molten chocolate, nail polish, foam and some suspensions. Magnetohydrodynamic (MHD) flows have importance in the engineering and industrial fields. These are used to control the flow and diffusion rate of neutrons in thermal nuclear reactors. Kudenatti et al. [11] presented MHD flow with the effect of suction/injection over a nonlinear stretching surface. Three-dimensional MHD flow with viscous dissipation and Joule heating is discussed by Hayat et al. [12]. Machireddy [13] analyzed magnetohydrodynamic flow past a vertical cylinder with chemical reactive species and radiation. MHD slip flow by a rotating permeable disk with variable properties is investigated by Rashidi et al. [14]. Hayat et al. [15] investigated heat transfer in third grade liquid between stretchable surfaces. Flow and transfer in electrically conducting liquid due to shrinking rotating disk is studied by Turkyilmazoglu [16]. Flow over a stretched surface remained a major area of study in many engineering and industrial problems due to its large applications. Examples include hot rolling, glass blowing, wire drawing, paper production, metal spinning and drawing of plastic films. The analysis of such flow problems are investigated by many researchers and scientists in various physical aspects. Ostwald-de Waele fluid flow over a stretching surface with variable fluid properties is carried out by Vajravelu et al. [17]. Hayat et al. [18] discussed heat transfer in a second grade liquid flow with Soret and Dufour effects. Flow of Casson fluid over a stretched surface with heat transfer and thermal radiation is presented by Bhattacharyya [19]. Hayat et al. [20] reported the unsteady MHD squeezing flow induced by a porous stretching plate. Presence of heat source/sink in the flow field gained importance because heat transfer rate and quality of final product depend on it. These effects remained prominent when dealing with chemical aspects and dissociating liquids. Turkyilmazoglu [21] presented unsteady radiative MHD flow over an impulsively started vertical plate with heat source and soret effects. Pavithra and Gireesha [22] examined the viscous dissipation effect on the Dusty fluid induced by exponentially stretched

* Corresponding author.
E-mail address: n_bkhan@yahoo.com (N.B. Khan).

https://doi.org/10.1016/j.rinp.2018.04.015
Received 7 January 2018; Received in revised form 30 March 2018; Accepted 8 April 2018
Available online 22 April 2018

Nomenclature

μ_B	plastic dynamic viscosity	R	radius of cylinder
p_y	yield stress of fluid	l	characteristics length
π	$e_{ij}e_{ij}$ with e_{ij} the (i,j)th component of deformation rate	β	Casson parameter
π_c	critical value of π	ΔT	characteristics temperature
u,v,w	velocity components	T	temperature
B_0	strength of magnetic field	T_∞	ambient temperature
r,ϕ,x	directions components	B_0	applied magnetic field
ν	kinematic viscosity	α	thermal diffusivity
ρ	density	γ	heat generation/absorption parameter
c_p	specific heat	Re	Reynold number
G	constant rotating speed of cylinder	Pr	Prandtl number
Q	coefficient of heat generation/absorption	M	magnetic parameter
H	strain rate at the surface of cylinder	β	Casson parameter
		$C_{fx},C_{f\phi}$	coefficients of surface drag force
		Nu	heat transfer rate

surface with heat absorption/generation. Magnetohydrodynamic (MHD) flow past an impermeable stretching surface subject to internal heat generation/absorption is reported by Parsa et al. [23]. Further relevant studies in this direction through the Refs. [24–30].

Literature survey indicates that two-dimensional flows over a stretched sheet were discussed extensively by various authors. However axisymmetric flow of non-Newtonian liquid induced by a swirling cylinder has not attained much attention of the researchers. Thus in this article we studied axisymmetric MHD flow of Casson fluid over a moving cylinder. Effects of heat generation/absorption are present. Variable temperature is considered at the surface. Governing nonlinear PDEs are transformed into the nonlinear ODEs using appropriate transformations. The resulting nonlinear system is solved by using built-in-Shooting [31–35]. Variation of different variables on the temperature, radial velocity, swirl velocity and axial velocity fields are examined. Skin friction coefficients and local Nusselt number are also numerically computed and discussed. Some studies regarding stretched surface are mentioned in Refs. [36–44]. Comparison of $f''(1)$ is also performed with the previous results [45].

Formulation

Consider axisymmetric flow of Casson liquid due to stretching and torsional motion of an impermeable cylinder. Heat transfer process is explored subject to heat absorption/generation. Thermal radiation and viscous dissipation effects are neglected. Assume that temperature is vary linearly of cylinder surface with axial distance (see Fig. 1).

Extra stress tensor for incompressible and isotropic Casson liquid flow is

$$S_{ij} = \begin{cases} \left(\mu_B + \frac{p_y}{\sqrt{2\pi}}\right)2e_{ij}, & \pi > \pi_c \\ \left(\mu_B + \frac{p_y}{\sqrt{2\pi_c}}\right)2e_{ij}, & \pi < \pi_c \end{cases} \tag{1}$$

Velocity and magnetic fields for the present flow field configuration are

$$V = [u(r,x),v(r,x),w(r,x)] \tag{2}$$

and

$$B = [B_0,0,0]. \tag{3}$$

Using Eq. (2) we obtain

$$\begin{bmatrix} 2\frac{\partial u}{\partial r} & \frac{\partial v}{\partial r}-\frac{v}{r} & \frac{\partial u}{\partial z}+\frac{\partial w}{\partial r} \\ \frac{\partial v}{\partial r}-\frac{v}{r} & 2\frac{u}{r} & \frac{\partial w}{\partial z} \\ \frac{\partial u}{\partial z}+\frac{\partial w}{\partial r} & \frac{\partial v}{\partial z} & 2\frac{\partial w}{\partial z} \end{bmatrix} \tag{4}$$

Present flow situation is governed by the following equations [26]:

$$\frac{\partial u}{\partial r} + \frac{\partial w}{\partial x} + \frac{u}{r} = 0, \tag{5}$$

$$u\frac{\partial u}{\partial r} + w\frac{\partial u}{\partial x} - \frac{v^2}{r} = -\frac{1}{\rho}\frac{\partial p}{\partial r} + \nu\left(1+\frac{1}{\beta}\right)\left(\frac{\partial^2 u}{\partial r^2} + \frac{1}{r}\frac{\partial u}{\partial r} + \frac{\partial^2 u}{\partial x^2} - \frac{u}{r^2}\right), \tag{6}$$

$$u\frac{\partial v}{\partial r} + w\frac{\partial v}{\partial x} + \frac{uv}{r} = \nu\left(1+\frac{1}{\beta}\right)\left(\frac{\partial^2 v}{\partial r^2} + \frac{1}{r}\frac{\partial v}{\partial r} + \frac{\partial^2 v}{\partial x^2} - \frac{v}{r^2}\right) - \frac{\sigma B_0^2 v}{\rho}, \tag{7}$$

$$u\frac{\partial w}{\partial r} + w\frac{\partial w}{\partial x} = -\frac{1}{\rho}\frac{\partial p}{\partial r} + \nu\left(1+\frac{1}{\beta}\right)\left(\frac{\partial^2 w}{\partial r^2} + \frac{1}{r}\frac{\partial w}{\partial r} + \frac{\partial^2 w}{\partial x^2}\right) - \frac{\sigma B_0^2 w}{\rho},$$

$$u\frac{\partial T}{\partial r} + w\frac{\partial T}{\partial x} = \alpha\left(\frac{\partial^2 T}{\partial r^2} + \frac{1}{r}\frac{\partial T}{\partial r} + \frac{\partial^2 T}{\partial x^2}\right) + \frac{Q_0}{\rho c_p}(T - T_\infty), \tag{8}$$

with

$$u(R,x) = 0,\quad v(R,x) = G,\quad w(R,x) = 2Hx,\quad T(R,x) = T_w(x) = T_\infty + \left(\frac{x}{l}\right)\Delta T,$$
$$u(r,x) \to 0,\quad w(r,x) \to 0,\quad T(r,x) \to T_\infty,\quad r \to \infty. \tag{9}$$

Applying

$$\eta = \left(\frac{r}{R}\right)^2,\quad u = -HR\frac{f(\eta)}{\sqrt{\eta}},\quad v = Gg(\eta),\quad w = 2Hxf'(\eta),\quad \theta(\eta) = \frac{T - T_\infty}{T_w - T_\infty}. \tag{10}$$

The continuity expression is fulfilled identically and remaining expressions (i.e. (6)–(9)) have the final forms:

$$\left(1+\frac{1}{\beta}\right)(\eta f''' + f'') + \mathrm{Re}(ff'' - f'^2) + \mathrm{Re}(ff'' - f'^2) - Mf' = 0, \tag{11}$$

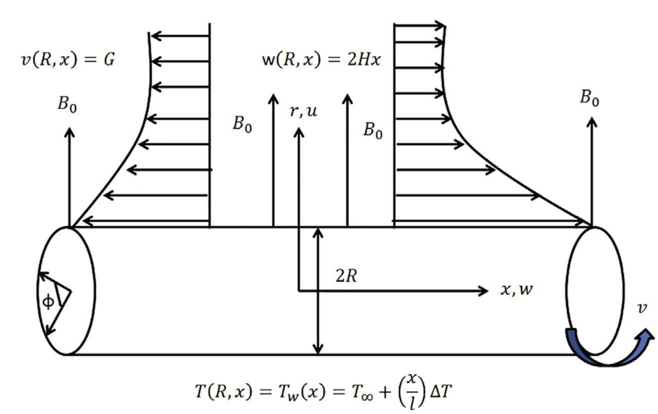

Fig. 1. Geometry of flow problem.

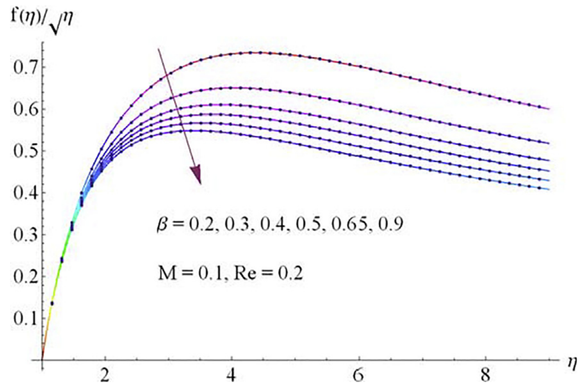

Fig. 2. β via $f(\eta)/\sqrt{\eta}$.

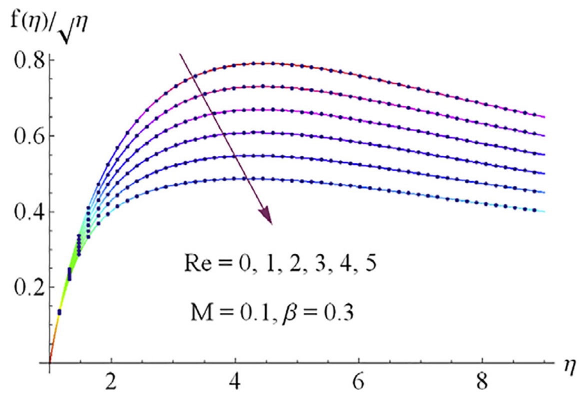

Fig. 3. Re via $f(\eta)/\sqrt{\eta}$.

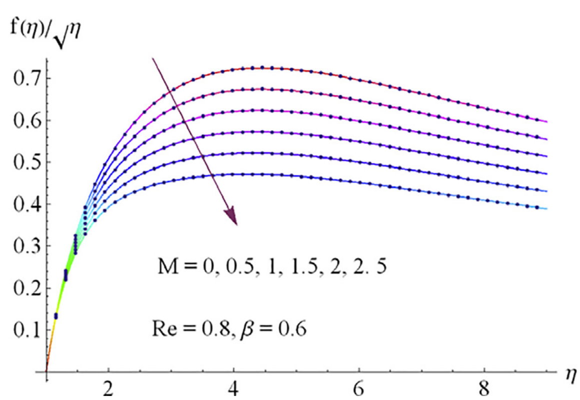

Fig. 4. M via $f(\eta)/\sqrt{\eta}$.

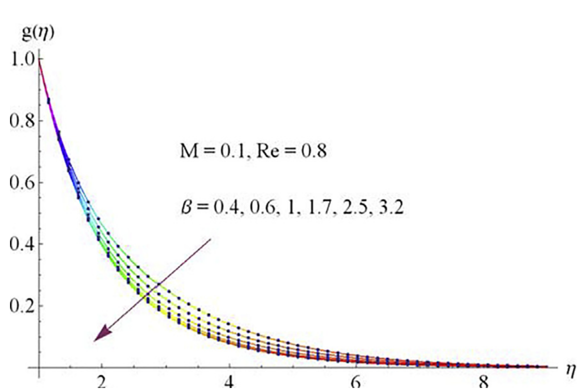

Fig. 5. β via $g(\eta)$.

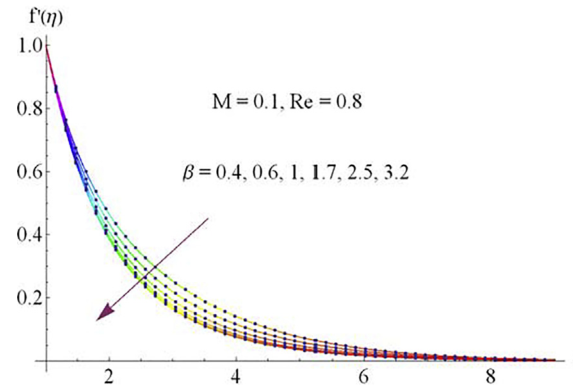

Fig. 6. β via $f'(\eta)$.

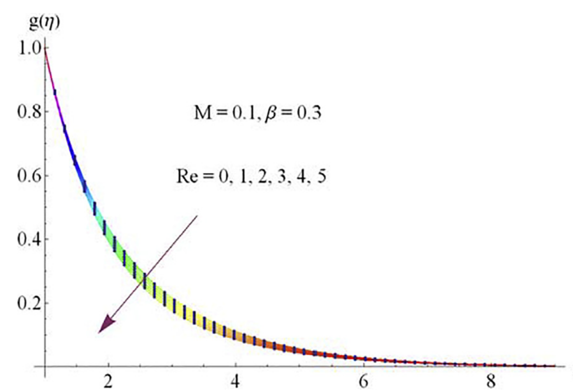

Fig. 7. Re via $g(\eta)$.

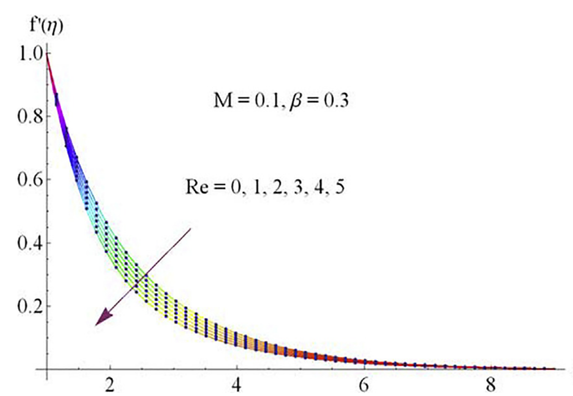

Fig. 8. Re via $f'(\eta)$.

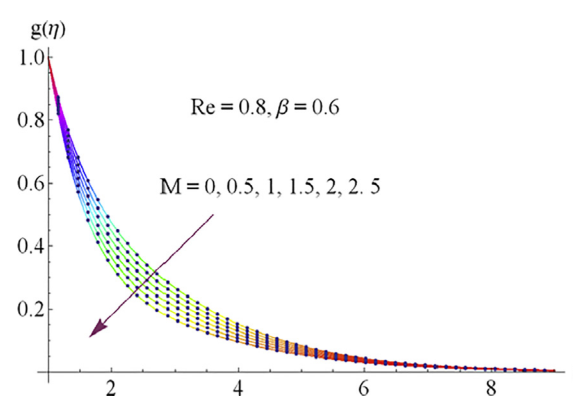

Fig. 9. M via $g(\eta)$.

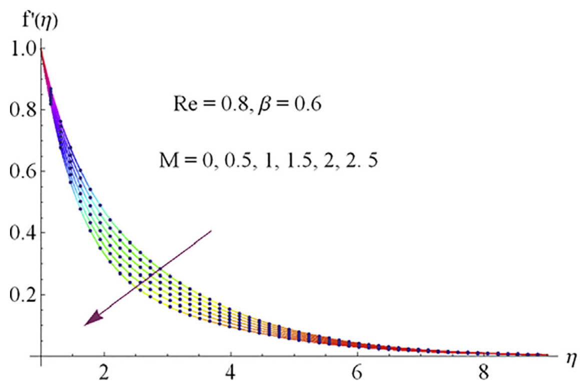

Fig. 10. M via $f'(\eta)$.

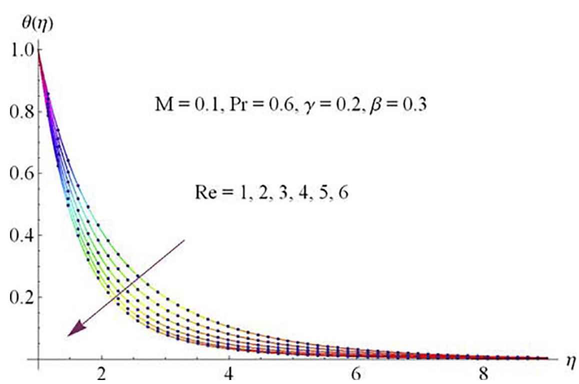

Fig. 11. Re via $\theta(\eta)$.

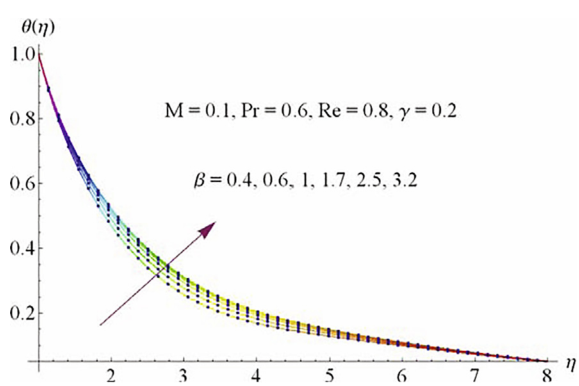

Fig. 12. β via $\theta(\eta)$.

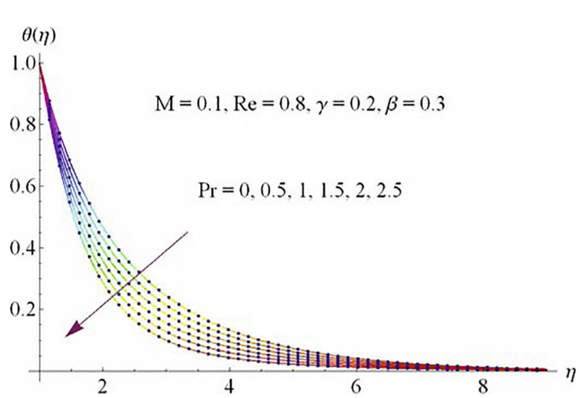

Fig. 13. Pr via $\theta(\eta)$.

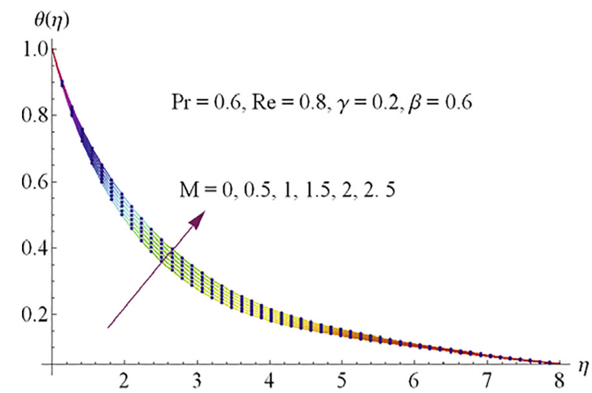

Fig. 14. M via $\theta(\eta)$.

Table 1
Comparison of $f''(1)$ with Ishak et al. [45] when $\frac{1}{\beta} \to 0$.

M	Re = 1		Re = 5	
	Ishak [45]	Present results	Ishak [45]	Present results
0	−1.1780	−1.1784	−2.4174	−2.4173
0.01	−1.1839	−1.1842	−2.4199	−2.4198
0.05	−1.2068	−1.2070	−2.4296	−2.4295
0.1	−1.2344	−1.2344	−2.4417	−2.4416
0.5	−1.4269	−1.4269	−2.5352	−2.5351

Table 2
Computational analysis of heat transfer rate and surface drag force subject to influential variables.

Re	β	M	Pr	γ	$-\theta'(1)$	$C_{fx}\ \mathrm{Re}\left(\frac{x}{R}\right)$	$C_{f\phi}\ \mathrm{Re}\left(\frac{G}{HR}\right)$
0.2	3	0.1	0.2	0.1	0.3562	−0.8876	−3.1650
0.4					0.3993	−1.0669	−3.2318
0.6					0.3443	−1.2143	−3.2972
	5				0.4395	−1.3032	−3.6519
	4				0.4301	−1.1685	−3.1191
	6				0.4265	−1.1216	−2.9505
		0.2			0.4170	−1.1918	−3.1565
		0.3			0.4091	−1.2564	−3.3343
		0.4			0.4024	−1.3164	−3.4894
			0.4		0.5077		
			0.6		0.6095		
			0.8		0.7076		
				0.1	0.7076		
				0.2	0.5416		
				0.8	0.3372		

$$\left(1+\frac{1}{\beta}\right)\left(\eta g''+g'-\frac{g}{4\eta}\right)+\mathrm{Re}\left(fg'-\frac{fg}{2\eta}\right)-Mg=0, \tag{12}$$

$$\eta\theta''+\theta'+\Pr\mathrm{Re}(f\theta'-f'\theta)+\Pr\mathrm{Re}\,\gamma\theta=0, \tag{13}$$

$$f(1)=0,\quad f'(1)=1,\quad g(1)=1,\quad \theta(1)=1,$$
$$f'(\infty)\to 0,\quad g(\infty)\to 0,\quad \theta(\infty)\to 0. \tag{14}$$

The parameter involves in flow problem have the following definitions

$$\gamma=\frac{Q}{2H\rho c_p},\quad \mathrm{Re}=\frac{HR^2}{2\nu},\quad M=\frac{\sigma B_0^2R^2}{4\nu\rho},$$
$$\beta=\mu_B\frac{\sqrt{2\pi_c}}{p_y},\quad \Pr=\frac{\nu}{\alpha}. \tag{15}$$

The pressure is independent of x under the present data. Since flow is axisymmetric so pressure can determined from Eq. (6) as follows:

$$p=A-\frac{H^2R^2\rho}{2\eta}f^2-2H\nu\left(1+\frac{1}{\beta}\right)f'+G^2\int_R^{\gamma}\frac{1}{t}g^2\left(\frac{t^2}{R^2}\right)dt. \tag{16}$$

Non-dimensional skin friction (C_{fx} and $C_{f\phi}$) coefficients and Nusselt (Nu_x) number are

$$C_{fx}\,\mathrm{Re}\left(\frac{x}{R}\right)=\left(1+\frac{1}{\beta}\right)f''(1), \tag{17}$$

$$C_{f\phi}\,\mathrm{Re}\left(\frac{G}{HR}\right)=\left(1+\frac{1}{\beta}\right)[2g'(1)-g(1)], \tag{18}$$

$$\frac{Nu}{2}=-\theta'(1). \tag{19}$$

Methodology and discussion

Built in routine of software Mathematica [43] for solving nonlinear ordinary differential equations subject to shooting method is utilized.

Variations of involved variables in the velocities ($f'(\eta)$,$g(\eta)$) and temperature $\theta(\eta)$ are discussed through this section. Characteristics of Casson (β) parameter on radial velocity ($f(\eta)/\sqrt{\eta}$) is exhibited in Fig. 2. Here ($f(\eta)/\sqrt{\eta}$) decreases for larger (β). With the increase of (β) the plastic dynamic viscosity increases which leads to reduce ($f(\eta)/\sqrt{\eta}$). It is also noted that fluid particles attain the velocity of the cylinder near the surface due to no slip condition. Velocity is higher near the cylinder and then it gradually decreases far away. Fig. 3 is interpreted to show the behavior of Reynolds number (Re) on ($f(\eta)/\sqrt{\eta}$). Velocity decreases with the increase of (Re). Velocity profile attains its maximum value near the cylinder and velocity gradually decays away from it. Fig. 4 displays significant feature of magnetic (M) parameter on ($f(\eta)/\sqrt{\eta}$). It is found that ($f(\eta)/\sqrt{\eta}$) decreases with the enhancement of (M). As (M) increases the Lorentz force is relatively higher than the viscous force. Since Lorentz force is a resistive force which offers resistance to the fluid motion. Therefore a decrease is noted in radial velocity for higher (M). Behavior of Casson parameter (β) on swirl and axial components of velocity fields is sketched in the Figs. 5 and 6. Both the velocity components are smaller for larger (β). Variation of (Re) on $g(\eta)$ and $f'(\eta)$ is displayed in the Figs. 7 and 8. Velocity components decrease gradually when Reynolds number (Re) increases. Analysis of (M) on velocity components is shown graphically in Figs. 9 and 10. Magnetic parameter (M) tends to decrease $g(\eta)$ and $f'(\eta)$. It is also scrutinized that fluid attains the maximum velocity at the surface. Behavior of Reynolds number (Re) on $\theta(\eta)$ is plotted in Fig. 11. Clearly $\theta(\eta)$ decays for larger (Re). Effect of (β) on the temperature profile is sketched in Fig. 12. Temperature profile is higher for larger (β). Influence of Prandtl (Pr) number on $\theta(\eta)$ is shown in Fig. 13. It is seen that $\theta(\eta)$ decays as (Pr) increases. As (Pr) increases volumetric heat capacity of the fluid increases which tends to decrease the temperature profile. Influence of $\theta(\eta)$ for various estimation of (M) is plotted in Fig. 14. Here $\theta(\eta)$ enhances for larger (M). Lorentz force is directly related to the magnetic parameter (M) which opposes velocity of fluid as a result more heat is produced. Hence temperature of the fluid increases. Comparison of $f''(1)$ with existing literature is shown (see Table 1). Present flow problem shows excellent agreement with previous results. Influence of different physical variables on the coefficients of drag force and heat transfer rate are shown in Table 2. Here increase of (Re) and (M) show the enhancement in the magnitude of axial drag force. However it shows decreasing effects for higher (β). Magnitude of $\left(C_{fx}\,\mathrm{Re}\left(\frac{x}{R}\right)\right)$ enhances for larger (Re) and (M) while it decays with the enhancement of (β). Nusselt number (Nu_x) enhances for higher (Re) and (Pr) while it shows decreasing behavior for larger (β), (M) and (γ).

Conclusion

Magnetohydrodynamic (MHD) flow of Casson liquid is studied in this article. Flow is caused due to torsional motion of cylinder. Heat transfer process is explored subject to heat absorption/generation. The main observations are as follows:

- All the velocity components are decreasing function of Casson parameter, Reynold number and magnetic parameter.
- Temperature is increasing function of (β), (M) and (γ) but it decays for larger (Re) and (Pr).
- Skin friction coefficients enhances for rising values of (Re), (M) while decreases for larger (β).
- Local Nusselt (Nu_x) number enhances for larger estimation of (Pr) and (Re) while it decays with (M), (β) and (γ).

References

[1] Fetecau C, Fetecau C, Jamil M, Mahmood A. Retraction note: flow of fractional Maxwell fluid between coaxial cylinders. Arch Appl Mech 2012;82:1003.

[2] Pramanik S. Casson fluid flow and heat transfer past an exponentially porous stretching surface in presence of thermal radiation. Ain Shams Eng J 2014;5:205–12.

[3] Shehzad SA, Alsaedi A, Hayat T, Alhuthali MS. Thermophoresis particle deposition in mixed convection three-dimensional radiative flow of an Oldroyd-B fluid. J Taiwan Inst Chem Eng 2014;45:787–94.

[4] Rashidi MM, Abelman S, FreidooniMehr N. Entropy generation in steady MHD flow due to a rotating porous disk in a nanofluid. Int J Heat Mass Transfer 2013;62:515–25.

[5] Mukhopadhyay S, Vajravelu K. Diffusion of chemically reactive species in Casson fluid flow over an unsteady permeable stretching surface. J Hydrody 2013;25(4):591–8.

[6] Turkyilmazoglu M, Pop I. Exact analytical solutions for the flow and heat transfer near the stagnation point on a stretching/shrinking sheet in a Jeffrey fluid. Int J Heat Mass Transfer 2013;57:82–8.

[7] Tripathi D, Bég OA. Transient magneto-peristaltic flow of couple stress biofluids: a magneto-hydro-dynamical study on digestive transport phenomena. Math Biosci 2013;246:72–83.

[8] Aziz T, Mahomed FM. Reductions and solutions for the unsteady flow of a fourth grade fluid on a porous plate. Appl Math Comput 2013;219:9187–95.

[9] Ramzan M, Farooq M, Alsaedi A, Hayat T. MHD three-dimensional flow of couple stress fluid with Newtonian heating. Eur Phys J Plus 2013;128:49.

[10] Ibrahim W, Shankar B, Nandeppanavar MM. MHD stagnation point flow and heat transfer due to nanofluid towards a stretching sheet. Int J Heat Mass Transfer 2013;56:1–9.

[11] Kudenatti RB, Kirsur SR, Achala LN, Bujurke NM. MHD boundary layer flow over a non-linear stretching boundary with suction and injection. Int J Non-linear Mech 2013;50:58–68.

[12] Hayat T, Naseem A, Farooq M, Alsaedi A. Unsteady MHD three-dimensional flow with viscous dissipation and Joule heating. Eur Phys J Plus 2013;128:158.

[13] Machireddy GR. Chemically reactive species and radiation effects on MHD convective flow past a moving vertical cylinder. Ain Shams Eng J 2013;4:879–88.

[14] Rashidi MM, Kavyani N, Abelman S. Investigation of entropy generation in MHD and slip flow over a rotating porous disk with variable properties. Int J Heat Mass Transfer 2014;70:892–917.

[15] Hayat T, Shafiq A, Alsaedi A, Awais M. MHD axisymmetric flow of third grade fluid between stretching sheets with heat transfer. Comput Fluids 2013;86:103–8.

[16] Turkyilmazoglu M. MHD flow and heat transfer due to shrinking rotating disk. Comput Fluids 2014;90:51–6.

[17] Vajravelu K, Prasad KV, Raju BT. Effects of variable fluid properties on the thin film flow of Ostwald-de Waele fluid over a stretching surface. J Hydrodyn 2013;25:10–9.

[18] Hayat T, Hussain M, Awais M, Obaidat S. Melting heat transfer in a boundary layer flow of a second grade fluid under Soret and Dufour effects. Int J Numer Methods Heat Fluid Flow 2013;23:1155–68.

[19] Bhattacharyya K. MHD stagnation point flow of Casson fluid and heat transfer over a stretching sheet with thermal radiation. J. Thermodyn. 2013;2013:169674.

[20] Hayat T, Qayyum A, Alsaedi A. MHD unsteady squeezing flow over a porous stretching plate. Eur Phys J Plus 2013;128:157.

[21] Turkyilmazoglu M. Soret and heat source effects on the unsteady radiative MHD free convection flow from an impulsively started infinite vertical plate. Int J Heat Mass Transfer 2012;55:7635–44.

[22] Pavithra GM, Gireesha BJ. Effect of internal heat generation/absorption on Dusty fluid flow over an exponentially stretching sheet with viscous dissipation. J Math 2013;2013:583615.

[23] Hayat T, Khan MI, Farooq M, Alsaedi A, Waqas M, Yasmeen T. Impact of Cattaneo-Christov heat flux model in flow of variable thermal conductivity fluid over a variable thicked surface. Int J Heat Mass Transfer 2016;99:702–10.

[24] Tamoor M, Waqas M, Khan MI, Alsaedi A, Hayat T. Magnetohydrodynamic flow of Casson fluid over a stretching cylinder. Results Phys 2017;7:498–502.

[25] Waqas M, Farooq M, Khan MI, Alsaedi A, Hayat T, Yasmeen T. Magnetohydrodynamic (MHD) mixed convection flow of micropolar liquid due to nonlinear stretched sheet with convective condition. Int J Heat Mass Transfer 2016;102:766–72.

[26] Khan MI, Waqas M, Hayat T, Alsaedi A. A comparative study of Casson fluid with homogeneous-heterogeneous reactions. J Colloid Interface Sci 2017;498:85–90.

[27] Sajid M, Hayat T. Influence of thermal radiation on the boundary layer flow due to an exponentially stretching sheet. Int Commun Heat Mass Transfer 2008;35:347–56.

[28] Hayat T, Khan MI, Farooq M, Yasmeen T, Alsaedi A. Stagnation point flow with

Cattaneo-Christov heat flux and homogeneous-heterogeneous reactions. J Mol Liq 2016;220:49–55.
[29] Hayat T, Sajid M. Analytic solution for axisymmetric flow and heat transfer of a second grade fluid past a stretching sheet. Int J Heat Mass Transfer 2007;50:75–84.
[30] Khan MI, Hayat T, Waqas M, Khan MI, Alsaedi A. Impact of heat generation/absorption and homogeneous-heterogeneous reactions on flow of Maxwell fluid. J Mol Liq 2017;233:465–70.
[31] Ali N, Sajid M, Abbas Z, Javed T. Non-Newtonian fluid flow induced by peristaltic waves in a curved channel. Eur J Mech B Fluids 2010;29:387–94.
[32] Hayat T, Khan MI, Waqas M, Alsaedi A. Mathematical modeling of non-Newtonian fluid with chemical aspects: a new formulation and results by numerical technique. Colloids Surf, A 2017;518:263–72.
[33] Hayat T, Khan MI, Waqas M, Alsaedi A, Farooq M. Numerical simulation for melting heat transfer and radiation effects in stagnation point flow of carbon-water nanofluid. Comput Methods Appl Mech Eng 2017;315:1011–24.
[34] Mustafa M, Hina S, Hayat T, Alsaedi A. Influence of wall properties on the peristaltic flow of a nanofluid: analytic and numerical solutions. Int J Heat Mass Transfer 2012;55:4871–7.
[35] Khan MI, Hayat T, Khan MI, Alsaedi A. A modified homogeneous-heterogeneous reactions for MHD stagnation flow with viscous dissipation and Joule heating. Int J Heat Mass Transfer 2017;113:310–7.
[36] Rehman KU, Saba NU, Malik MY, Zehra I. Nanoparticles individualities in both Newtonian and Casson fluid models by way of stratified media: a numerical analysis. Euro Phys J E 2018;41:37.
[37] Khan I, Rehman KU, Malik MY. A computational analysis on homogeneous-heterogeneous mechanism in Carreau fluid flow. Results Phys 2018;8:1028–33.
[38] Rehman KU, Malik AA, Tahir M, Malik MY. Undersized description on motile gyrotactic micro-organisms individualities in MHD stratified water-based Newtonian nanofluid. Results Phys 2018;8:981–7.
[39] Rehman KU, Malik MY, Khan AA, Zehra I, Zahri M, Tahir M. Numerical solution of chemically reactive non-Newtonian fluid flow: dual stratification. Euro Phys J Plus 2017;132:550.
[40] Waqas M, Farooq M, Khan MI, Alsaedi A, Hayat T, Yasmeen T. Magnetohydrodynamic (MHD) mixed convection flow of micropolar liquid due to nonlinear stretched sheet with convective condition. Int J Heat Mass Transfer 2016;102:766–72.
[41] Hayat T, Khan MI, Qayyum S, Alsaedi A. Entropy generation in flow with silver and copper nanoparticles. Colloids Surf, A 2018;539:335–46.
[42] Khan MI, Hayat T, Khan MI, Alsaedi A. Activation energy impact in nonlinear radiative stagnation point flow of Cross nanofluid. Int Commun Heat Mass Transfer 2018;91:216–24.
[43] Khan MWA, Khan MI, Hayat T, Alsaedi A. Entropy generation minimization (EGM) of nanofluid flow by a thin moving needle with nonlinear thermal radiation. Physica B 2018;534:113–9.
[44] Hayat T, Khan MI, Qayyum S, Alsaedi A, Khan MI. New thermodynamics of entropy generation minimization with nonlinear thermal radiation and nanomaterials. Phys Lett A 2018;382:749–60.
[45] Ishak A, Nazar R, Pop I. Magnetohydrodynamic (MHD) flow and heat transfer due to a stretching cylinder. Energy Convers Manage 2008;49:3265–9.